Journal of the Serbian Chemical Society
JSCS@tmf.bg.ac.rs • www.shd.org.rs/JSCS

J. Serb. Chem. Soc. 75 (6) 773–788 (2010)
JSCS–4006

UDC 546.562'472+542.913+
547.477.2+547.963.32:615.28
Original scientific paper

Synthesis, characterization, DNA interaction and antimicrobial screening of isatin-based polypyridyl mixed-ligand Cu(II) and Zn(II) complexes

NATARAJAN RAMAN* and SIVASANGU SOBHA

Research Department of Chemistry, VHNSN College, Virudhunagar-626 001, India

(Received 20 October 2009, revised 17 March 2010)

Abstract: Several mixed ligand Cu(II)/Zn(II) complexes using 3-(phenylimino)-1,3-dihydro-2*H*-indol-2-one (obtained by the condensation of isatin and aniline) as the primary ligand and 1,10-phenanthroline (phen)/2,2'-bipyridine (bpy) as an additional ligand were synthesized and characterized analytically and spectroscopically by elemental analyses, magnetic susceptibility and molar conductance measurements, as well as by UV–Vis, IR, NMR and FAB mass spectroscopy. The interaction of the complexes with calf thymus (CT) DNA was studied using absorption spectra, cyclic voltammetric and viscosity measurements. They exhibit absorption hypochromicity, and the specific viscosity increased during the binding of the complexes to calf thymus DNA. The shifts in the oxidation–reduction potential and changes in peak current on addition of DNA were shown by CV measurements. The Cu(II)/Zn(II) complexes were found to promote cleavage of pUC19 DNA from the supercoiled form I to the open circular form II and linear form III. The complexes show enhanced antifungal and antibacterial activities compared with the free ligand.

Keywords: 1,10-phenanthroline/2,2'-bipyridine; Cu(II) and Zn(II) complexes; antimicrobial activity; DNA binding and cleavage.

INTRODUCTION

The therapeutic and diagnostic properties of transition metal complexes have attracted considerable attention leading to their application in many areas of modern medicine.[1] Many coordination compounds of transition metal ions accomplish nucleolytic cleavage.[2] In this regard, mixed-ligand metal complexes were found to be particularly useful because of their potential to bind DNA *via* a multitude of interactions and to cleave the duplex by virtue of their intrinsic chemical, electrochemical, and photochemical reactivities.[3–8] A recent study on the incorporation of good intercalators, such as phen (1,10-phenanthroline), bpy

* Corresponding author. E-mail: drn_raman@yahoo.co.in
doi: 10.2298/JSC091020054R

(2,2'-bipyridine), *etc.* found high affinity between DNA base pairs and their planar structure through stacking interaction.[9] A singular advantage in the use of these metallo-intercalators for such studies is that the ligands or the metal ion in them can be varied in an easily controlled manner to facilitate individual applications.[10,11] Although DNA interactions of number of mixed-ligand complexes previously appeared in the literature, there is still scope to design and study isatin-based Schiff base containing 1,10-phenantroline/2,2'-bipyridine with the Cu(II) and Zn(II) as new chemical nucleases. Bearing these facts in mind, the nuclease activity of mixed-ligand complexes of Cu(II) and Zn(II) containing 1,10-phenantroline/2,2'-bipyridine is reported herein. DNA binding was also researched. Hence, the present study is very valuable in understanding the mode of complex binding to DNA, as well as laying the foundation for the rational design of DNA structure probes and antitumor drugs.

EXPERIMENTAL

All chemicals used in the present work, *viz.*, isatin, aniline, 1,10-phenanthroline, 2,2'-bipyridine and copper and zinc chlorides were of analytical reagent grade (produced by Merck, Germany). Commercial solvents were distilled and then used for the preparation of the ligand and its complexes. CT DNA and pUC19 DNA was purchased from Bangalore Genei (India). Microanalyses (C, H and N) were performed using a Carlo Erba 1108 analyzer at the sophisticated analytical instrument facility (SAIF), Central Drug Research Institute (CDRI), Lucknow, India. Molar conductivities in DMSO (10^{-2} mol/dm^3) at room temperature were measured using a Systronic model-304 digital conductivity meter. Magnetic susceptibility measurements of the complexes were realized by a Gouy balance using copper sulfate pentahydrate as the calibrant. The IR spectra were recorded on a Perkin–Elmer 783 spectrophotometer in the 4000–400 cm^{-1} range using KBr pellets. The NMR spectra were recorded on a Bruker Avance Dry 300 FT-NMR spectrometer in DMSO-d_6 with TMS as the internal reference. The FAB-MS spectra were recorded using a VGZAB-HS spectrometer at room temperature in a 3-nitrobenzyl alcohol matrix. Electron paramagnetic resonance spectra (EPR) of the mixed ligand complexes of copper(II) were recorded on a Varian E 112 EPR spectrometer in DMSO solution both at room temperature and liquid nitrogen temperature (77 K) using TCNE (tetracyanoethylene) as the g-marker. The absorption spectra were recorded using a Shimadzu model UV-1601 spectrophotometer at room temperature. Electrochemical studies were realized using a CHI Electrochemical analyzer, controlled by CHI620C software. The CV measurements were performed using a glassy carbon working electrode and an Ag/AgCl reference electrode (all potentials refer to this reference electrode) and the supporting electrolyte was 50 mmol/L NaCl–5 mmol/L Tris-HCl buffer (pH 7.2). All solutions were deoxygenated by purging with N_2 for 30 min prior to the measurements.

Preparation of ligand (L)

The Schiff base was synthesized according to a literature procedure.[12] A methanolic solution of aniline (0.040 mol, 3.65 mL) was added to a methanolic solution (25 mL) of isatin (0.040 mol, 5.8 g) and the reaction mixture was refluxed for *ca.* 6 h. The end of the reaction was monitored by TLC. In this technique, a small quantity of a solution of the Schiff base to be analyzed was deposited as a small spot on a TLC plate which had a thin layer of silica gel

(SiO_2) coated on a glass plate as the absorbent. It was used as the stationary phase and the mobile phase was toluene:ethanol (9:1). The observed R_f value was 0.68.

The formed yellowish orange product (L) was filtered and washed with methanol and dried *in vacuo*. Yield: 86 %. The preparation of the Schiff base is schematically presented in Fig. 1.

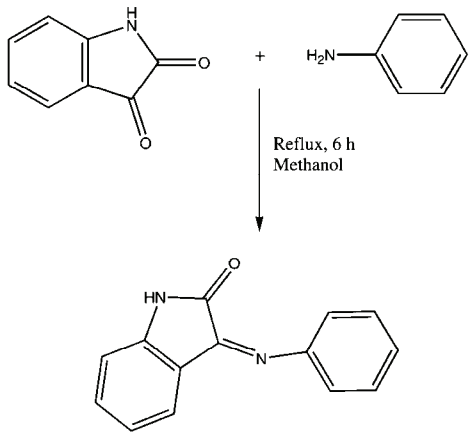

Fig. 1. Synthesis of the Schiff base.

Synthesis of the $[ML(Phen)_2]Cl_2$/$[ML(bpy)_2]Cl_2$ complexes

The complexes were prepared by mixing the appropriate molar quantities of the ligand and the metal salts using the following procedure. A methanolic solution of Schiff base (0.0030 mol) was stirred with a methanolic solution (5 mL) of the required anhydrous metal(II) chloride (0.0030 mol) for *ca.*1 h. To the above mixture, a methanolic solution (5 mL) of 1,10-phenanthroline (phen)/2,2'-bipyridine (bpy) (0.0060 mol) was added in a 1:1:2 molar ratio and the stirring was continued for *ca*. 1 h. The obtained solid product was filtered and washed with methanol.

DNA binding experiments

The interactions between the metal complexes and DNA were studied using electrochemical and electronic absorption methods. The disodium salt of calf thymus DNA was stored at 4 °C. A solution of DNA in the buffer 50 mmol/L NaCl–5 mmol/L Tris-HCl (pH 7.2) in water gave a ratio 1.9 of the UV absorbance at 260 and 280 nm, A_{260}/A_{280}, indicating that the DNA was sufficiently free from protein.[13] The concentration of DNA was measured using its extinction coefficient at 260 nm (6600 mol^{-1} L cm^{-1}) after a 1:100 dilution. Stock solutions were stored at 4 °C and used no more than 4 days. Doubly distilled water was used to prepare the solutions. Concentrated stock solutions of the complexes were prepared by dissolving the complexes in DMSO and diluting suitably with the corresponding buffer to the required concentration for all the experiments. The data were then fitted to Eq. (1) to obtain the intrinsic binding constant (K_b) values for the interaction of the complexes with DNA:

$$[DNA]/(\varepsilon_a - \varepsilon_f) = [DNA]/(\varepsilon_b - \varepsilon_f) + 1/K_b(\varepsilon_b - \varepsilon_f) \quad (1)$$

where ε_a, ε_f, and ε_b are the apparent, free and bound metal complex extinction coefficients, respectively. A plot of $[DNA]/(\varepsilon_b - \varepsilon_f)$ *vs*. [DNA] gave a slope of $1/(\varepsilon_b - \varepsilon_f)$ and a *y*-intercept equal to $[K_b/(\varepsilon_b - \varepsilon_f)]^{-1}$; thus, K_b is the ratio of the slope to the *y*-intercept. Viscosity mea-

surements at room temperature were performed using a semi-micro dilution capillary viscometer. Each experiment was performed three times and an average flow time was calculated. The data are presented as $(\eta/\eta_0)^{1/3}$ *vs*. the binding ratio, where η is the viscosity of a DNA solution in the presence of a complex and η_0 is the viscosity of DNA in solution alone.

pUC19 DNA cleavage study

The cleavage of pUC19 DNA was determined by agarose gel electrophoresis. The gel--electrophoresis experiments were performed by incubation of the samples containing 30 μmol/L pUC19 DNA, 50 μmol/L copper complex and 50 μmol/L hydrogen peroxide (H_2O_2) in Tris-HCl/NaCl buffer (pH 7.2) at 37 °C for 2 h. After incubation, the samples were electrophoresed for 2 h at 50 V on 1 % agarose gel using Tris-acetic acid–EDTA buffer (pH 7.2). The gel was then stained using 1 μg cm^{-3} ethidium bromide (EB) and photographed under 360 nm ultraviolet light. All experiments were performed at room temperature unless otherwise stated.

Antimicrobial activity studies

The *in vitro* antibacterial activity of the ligand and its complexes were tested against the bacteria *Staphylococcus aureus*, *Pseudomonas aeruginosa*, *Escherichia coli*, *Staphylococcus epidermidis*, *Klebsiella pneumoniae* by the paper disc method using nutrient agar as the medium. The antifungal activity was evaluated by the paper disc method against the fungi *Aspergillus niger*, *Fusarium solani*, *Culvularia lunata*, *Rhizoctonia bataticola* and *Candida albicans* cultured on potato dextrose agar medium. Streptomycin and nystatin were used as standards for bacteria and fungi, respectively. A stock solution (10^{-2} mol L^{-1}) was prepared by dissolving the compound in DMSO and the solution was serially diluted in order to find the minimum inhibitory concentration *(MIC)* value. Test extract loaded discs inoculated with microorganisms were incubated at 30 °C for 24 h for the bacteria and 72 h for fungi. During the incubation period, the test solution diffused and the growth of the inoculated microorganisms was affected. The concentration at which an inhibition zone developed was noted.

RESULTS AND DISCUSSION

The ligand (L) and the mixed ligand complexes containing L and phen/bpy were stable in air. L is soluble in common organic solvents but the complexes are soluble only in DMF and DMSO. Elemental analyses of L and the complexes were in agreement with the assigned formula. The higher molar conductance values of the complexes in DMSO show their electrolytic nature. The elemental analysis and FAB-mass data, together with other properties, are given in Table I.

Mass spectra

The FAB-mass spectra of L and its complexes having phen were recorded and the obtained molecular ion peaks confirmed the proposed formulae. The mass spectrum of L ($C_{14}H_{10}N_2O$) exhibited peaks at 222 (M^+), 223 (M+1) and 224 (M+2) with 68, 100 and 49 % abundances, respectively. The most abundant peak at *m*/*z* 223 represents the molecular ion peak of L. The mass spectrum of the copper complex $[CuC_{38}H_{26}N_6O]Cl_2$ showed peaks at 717 (M^+), 718 (M+1), 719 (M+2) with 8.7, 9.2 and 9.9 % abundances, respectively. The most abundant peak at *m*/*z* 719 represents the molecular ion peak of the complex and the other peaks are isotopic species. In addition, the spectrum exhibited fragments at *m/z*

180 and 77, which represent phen and phenyl moieties, respectively. The *m*/*z* of all the fragments of L and the mixed ligand complexes, together with the relative intensities confirmed the stoichiometry of the complexes to be of the type $[ML(phen)_2/(bpy)_2]Cl_2$ (where L = isatin-based Schiff base).The structural formulas of the complexes are shown in Fig. 2. Thus, the mass spectral data reinforced the conclusion drawn from the analytical and conductance values.

TABLE I. Physical and analytical data of the synthesized Schiff base and its complexes

Compound	Yield %	Color	Found (Calcd.), %				MW	Λ_M S cm^2 mol^{-1}	μ_{eff} / μ_B
			M	C	H	N			
L	86	Yellowish orange	–	72.7 (72.9)	5.0 (5.0)	14.1 (14.4)	222.0	–	–
$[CuL(phen)_2]Cl_2$	71	Pale green	8.8 (8.5)	63.6 (63.1)	3.6 (3.5)	11.7 (11.2)	717.1	104.5	1.89
$[CuL(bpy)_2]Cl_2$	67	Pale green	9.5 (8.9)	61.0 (59.2)	3.9 (3.3)	12.5 (12.1)	669.0	115.2	1.86
$[ZnL(phen)_2]Cl_2$	79	Pale brown	9.0 (8.7)	63.4 (59.7)	3.6 (3.1)	11.6 (11.4)	718.9	102.9	Diamagnetic
$[ZnL(bpy)_2]Cl_2$	83	Pale brown	9.7 (9.3)	60.8 (60.6)	3.9 (3.8)	12.5 (12.0)	670.9	112.6	Diamagnetic

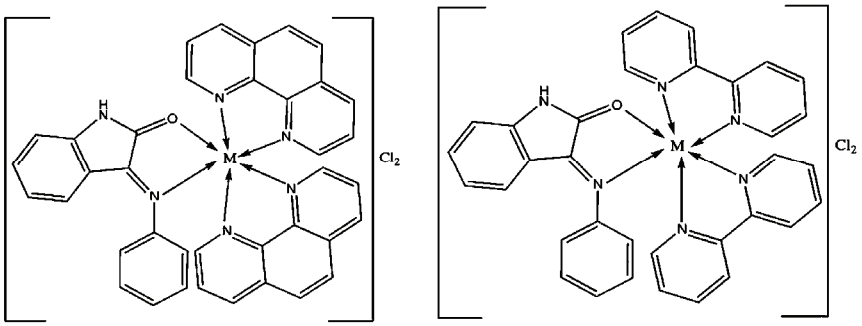

(a) (b)

Fig. 2. The structural formulas of the complexes a) $[ML(phen)_2]Cl_2$ and b) $[ML(bpy)_2]Cl_2$; M = Cu(II) or Zn(II).

IR Spectra

The IR spectrum of the free ligand (L) showed a broad band around 3257 cm^{-1}, which can be attributed to NH stretching vibration of the isatin moiety. The position of this band remained at nearly the same frequency in spectra of the metal complexes, suggesting the uncoordination of this group. The band at 1763 cm^{-1} in the spectrum of the free ligand, assigned to $\nu_{C=O}$ of isatin moiety, shifted towards lower values, around 1719–1710 cm^{-1}, in the complexes, indicating the coordination of the carbonyl oxygen atom of the isatin residue. The C=N stretching frequency of the Schiff base ligand appears in the region 1613–1608 cm^{-1},

which was shifted towards lower values in all the complexes, indicating the involvement of the –C=N nitrogen in coordination to the central metal ion. All the complexes showed bands in the regions 1090–1100 and 700–750 cm^{-1}. These can be assigned to phen/bpy ring –C–H and –C=N stretching vibrations, respectively. The appearance of two new bands in the regions 486–472 and 547–533 cm^{-1} in the spectra of the complexes, due to ν_{M-N} and ν_{M-O} stretching vibrations, respectively, also confirmed the formation of metal complexes. The characteristic IR data are presented in Table II.

TABLE II. IR spectral data (cm^{-1}) of the ligand and its complexes

Compound	ν_{N-H}	$\nu_{C=O}$	$\nu_{C=N}$	ν_{M-N}	ν_{M-O}
L	3257	1763	1645	–	–
$[CuL(phen)_2]Cl_2$	3262	1711	1613	472	533
$[CuL(bpy)_2]Cl_2$	3267	1710	1608	481	536
$[ZnL(phen)_2]Cl_2$	3268	1717	1611	476	537
$[ZnL(bpy)_2]Cl_2$	3265	1719	1619	486	547

^{1}H-NMR Spectra

^{1}H-NMR (300 MHz, DMSO-d_6, δ / ppm) spectrum of the Schiff base exhibited the following signals: the signal at 10.92 (1H, *s*) was assigned to the NH proton of isatin and the multiplet signal around 6.43–7.10 (4H, *m*) to aromatic protons. In addition to these, one singlet peak observed at 7.21 was ascribed to aniline ring protons. In the ^{1}H-NMR spectra of the Zn(II) complexes, the protons of L are shifted downfield due to coordination to the metal ions. The resonance peaks observed in the spectrum of the $[ZnL(phen)_2]Cl_2$ complex at 7.34–7.40 and 7.81–8.37 were assigned to phen protons and the signals at 7.54–7.73 and 8.23––8.37 in the spectrum of $[ZnL(bpy)_2]Cl_2$ were assigned to bpy protons.

EPR Spectra

The EPR spectra of the copper complexes exhibited an auxiliary symmetric g-tensor parameters with $g_\parallel > g_\perp > 2.0023$, indicating that the copper site had a $d_{x^2}–d_{y^2}$ ground state, characteristic of octahedral geometry.[14] According to Hathaway,[15] if the value of *G* is greater than four, the exchange interaction between the copper(II) centers in the solid state is negligible, whereas when *G* is less than four, there is considerable exchange interaction from the polypyridyl nitrogen atom. The *G* values calculated for the present copper complexes lie within the range 2.936–3.277, which are consistent with a $d_{x^2}–d_{y^2}$ ground state.

Apart from this, the covalency parameters α^2 (covalent in-plane σ-bonding) and β^2 (covalent in-plane π-bonding) were calculated using a simplified MO theory and the results are summarized in Table III.

The α^2 and β^2 values indicated a greater interaction in the in-plane π-bonding than in the covalent in-plane σ-bonding, whereas the in-plane π-bonding is

almost ionic. The higher value of α^2 compared to β^2 indicates that the in-plane σ-bonding is more covalent than the in-plane π-bonding. Based on these observations, a distorted octahedral geometry is proposed for both the copper complexes.

TABLE III. The spin Hamiltonian parameters of the copper complexes in DMSO solution at 300 and 77 K

Compound	$g_{\parallel}$	$g_{\perp}$	$A_{\parallel}\times10^4$ / cm^{-1}	$A_{\perp}\times10^4$ / cm^{-1}	α^2	β^2	G
$[CuL(phen)_2]Cl_2$	2.232	2.071	169.0	66.0	0.767	0.615	3.2
$[CuL(bpy)_2]Cl_2$	2.351	2.072	171.3	64.3	0.724	0.518	2.9

Electronic absorption spectra

The UV–Vis spectra of the copper complexes were recorded in DMSO solution. They show a d–d band at around 734–737 nm. This band may be assigned to $^2E_g \rightarrow {}^2T_{2g}$ transitions, characteristics for a distorted octahedral structure. In addition, the complexes exhibited intense bands in the 395–398 nm region, which are attributed to charge transfer transitions. The intense higher energy bands at around 272 and 285 nm can be attributed to intra-ligand π–π* transitions. The copper complexes showed magnetic moment values in the range of 1.87–1.89 μ_B which indicate the monomeric nature of the complexes. The zinc(II) complexes showed bands at 375 and 378.5 nm, assigned to intra-ligand charge transfer transitions. They are diamagnetic.

Based on the elemental analysis, magnetic moments, mass, EPR spectra, electronic, IR and ^{1}H-NMR data, the proposed structures of the complexes are given in Fig. 2.

CT-DNA binding studies

Electronic absorption titration. The binding interaction of the metal complexes with DNA was monitored by UV–Vis spectroscopy. The absorption spectra of the complexes in the presence or without DNA were mutually compared, which is shown in Fig. 3. In the UV region of the spectra, all the copper complexes exhibited an intense absorption around 395–398 nm and zinc complexes showed a band at 375–378.5 nm, which are attributed to n–π* transitions. With increasing concentration of DNA, both the copper and zinc complexes showed hypochromicity and a red-shifted charge transfer peak maxima in the absorption spectra.

The hypochromicity values of the complexes $[CuL(phen)_2]Cl_2$, $[CuL(bpy)_2]Cl_2$, $[ZnL(phen)_2]Cl_2$ and $[ZnL(bpy)_2]Cl_2$ observed in the presence of DNA were 2.16, 1.08, 1.07 and 1.05 respectively, and their hypsochromic shifts were 8.6, 4.2 and 4.0, 5.6 nm, respectively. The change in the absorbance values with increasing amount of DNA was used to evaluate the intrinsic binding constant K_b for the present complexes, the values of which are given in Table IV. The change in hypochromicity may be attributed to the nature of the binding of

the mixed ligand complexes with DNA, which is significant due to π-stacking or hydrophobic interactions of the aromatic phenyl rings. However, the metal ions play crucial role in DNA binding by these complexes. In general, the DNA binding abilities seem to follow the order: $[CuL(phen)_2]Cl_2$ > $[CuL(bpy)_2]Cl_2$ > > $[ZnL(bpy)_2]Cl_2$ > $[ZnL(phen)_2]Cl_2$. The high binding nature of the metal complexes may be due to additional π-π interaction through the aromatic phenyl rings.

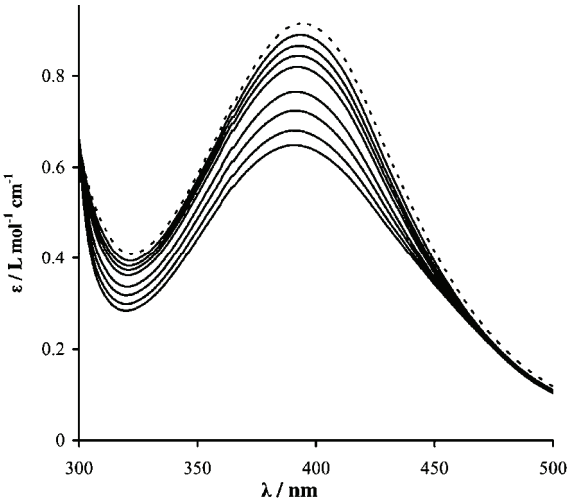

Fig. 3. Electronic absorption spectrum of $[CuL(phen)_2]$ in the absence (dash line) and presence (dark line) of different concentrations (0 to 400 μM) of DNA.

TABLE IV. Electronic absorption spectral properties of the Cu(II) and Zn(II) complexes

Compound	λ_{max} / nm		$\Delta\lambda_{max}$ / nm	H / %	$K_b \times 10^{-5}$ / mol^{-1} dm^3
	Free	Bound			
$[CuL(phen)_2]Cl_2$	397.8	389.2	8.6	2.16	5.84
$[CuL(bpy)_2]Cl_2$	393.2	389.0	4.2	1.08	5.36
$[ZnL(phen)_2]Cl_2$	375.0	371.0	4.0	1.07	2.74
$[ZnL(bpy)_2]Cl_2$	378.4	372.8	5.6	1.50	3.34

Viscosity studies. A useful technique to prove intercalation is viscosity measurements, which are sensitive to change in length of the DNA and are regarded as the least ambiguous and the most critical tests of binding mode in solution in the absence of crystallographic structural data or NMR spectra.[16] Under appropriate conditions, intercalation of drugs, such as ethidium bromide [EB], causes a significant increase in the viscosity of a DNA solution due to the increase in the separation of the base pairs of the intercalation sites and hence, result in an increase in the overall DNA contour length, as shown in Fig. 4. On the other hand, drug molecular binding exclusively in the DNA grooves causes a less pronounced or no changes in the viscosity of a DNA solution.[17] The viscosity of the DNA solution increased with increasing ratio of both the copper and zinc complexes to DNA. This result further suggests an intercalating binding mode of the

complexes with DNA and also parallels the above spectroscopic results, such as hypochromism and bathochromism of the complexes in the presence of DNA.

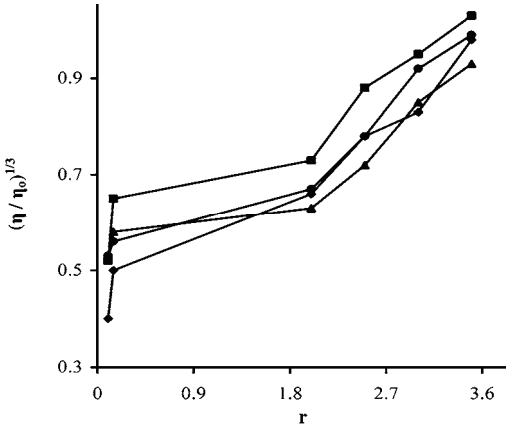

Fig.4. Change in the relative viscosity $(\eta/4_0)^{1/3}$ of CT DNA as a function of *r*, the molar ratio of the compound to the DNA base pairs. The effect of increasing amounts of:
$[CuL(phen)_2]Cl_2$ (▲),
$[CuL(bpy)_2]Cl_2$ (■),
$[ZnL(phen)_2]Cl_2$ (♦) and
$[ZnL(bpy)_2]Cl_2$ (●)
on the relative viscosity of DNA.

Redox studies. The application of cyclic voltammetry to the studies of the complexes bound to DNA provides a useful complement to the previously used investigation methods, *i.e.*, UV–Vis spectroscopy and viscosity measurements. The cyclic voltammograms of the glassy carbon electrode in solutions containing $[CuL(phen)_2]Cl_2$ in the absence and in the presence of varying amounts of DNA are shown in Fig. 5.

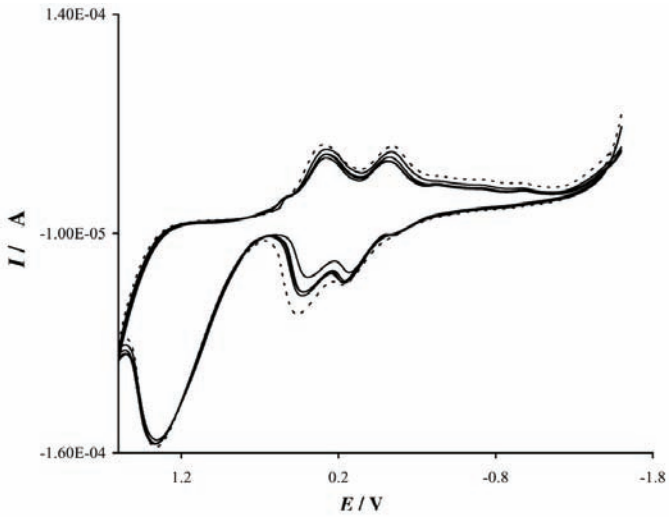

Fig.5. Cyclic voltammograms of the glassy carbon electrode in solutions containing $[CuL(phen)_2]Cl_2$ in the absence (dash line) and presence (dark lines) of different concentrations (0 to 400 μM) of DNA.

In the absence of DNA, the first redox couple cathodic peak appeared at 0.29 V for Cu(III) → Cu(II) (E_{pa} = 0.49 V, E_{pc} = 0.29 V, ΔE_p = 0.20 V, and $E_{1/2}$ = = 0.39 V) and the second redox couple cathodic peak appeared at –0.16 V for Cu(II) → Cu(I), (E_{pa} = 0.17 V, E_{pc} = –0.16 V, ΔE_p = 0.33 V, and $E_{1/2}$ = 0.17 V). The ratio of cathodic to anodic peak currents, I_{pa}/I_{pc} = 0.95, indicated a quasi-reversible redox process. The formal potential ($E_{1/2}$), taken as the average of E_{pc} and E_{pa}, was 0.39 V for the first redox couple in the absence of DNA. The presence of DNA in the solution at the same concentration as $[CuL(phen)_2]Cl_2$ caused a negative shift in the potential ΔE_p by 0.160 V and a decrease in $E_{1/2}$ by 0.35 V, Table V. The value of I_{pa}/I_{pc} also decreased with increasing DNA concentration. The decrease of the anodic and cathodic peak currents of the complex in the presence DNA is due to a decrease in the apparent diffusion coefficient of the Cu(II) complex upon complexation with the DNA macromolecules. These results show that $[CuL(phen)_2]Cl_2$ stabilizes the duplex (GC pairs) by intercalation.

TABLE V. Electrochemical parameters for the interaction of DNA with the Cu(II) complexes

Compound	Redox couple	$E_{1/2}$ / V		ΔE_p / V		K_+/K_{2+}	I_{pc}/I_{pa}
		Free	Bound	Free	Bound		
$[CuL(phen)_2]Cl_2$	Cu(III) → Cu(II)	0.39	0.35	0.20	0.16	0.0965	0.95
	Cu(II) → Cu(I)	0.005	0.014	0.33	0.28	0.4081	0.93
$[CuL(bpy)_2]Cl_2$	Cu(III) → Cu(II)	0.42	0.27	0.16	0.14	0.0826	0.84
	Cu(II) → Cu(I)	0.02	0.07	0.06	0.12	0.7042	0.75

Considering the CV behavior of the glassy carbon electrode in solutions containing $[CuL(bpy)_2]Cl_2$ in the absence of DNA, the first redox couple cathodic peak appeared at 0.338 V for Cu(III) → Cu(II), (E_{pa} = 0.50 V, E_{pc} = 0.34 V, ΔE_p = 0.16 V and $E_{1/2}$ = 0.42 V), while the second cathodic peak appeared at 0.17 V for Cu(II) → Cu(I) (E_{pa} = 0.23 V, E_{pc} = 0.17 V, ΔE_p = 0.06 V and $E_{1/2}$ = = 0.20 V). The I_{pa}/I_{pc} ratios of these two redox couples were approximately unity. This indicates that the reaction of the complex on the working electrode surface was a quasi-reversible redox process. The incremental addition of DNA to the complex caused a negative shift in the potential of the second cathodic peak and a decrease in the current intensity. The changes in the voltammetric currents in the presence of CT DNA can be attributed to the slow diffusion of the metal complex bound to the large, slowly diffusing DNA molecule. The changes of the peak currents observed for the complexes upon addition of CT DNA may indicate that the complexes possess a higher DNA binding affinity. The results lead conclusions similar to those deduced from the spectroscopic and viscosity data of the complexes in the presence of DNA.

The Zn(II) complexes showed only a reduction peak from –0.99 to –0.80 V (E_{pc}) and no oxidation peak in the absence of DNA. The incremental addition of DNA to the Zn(II) complexes increased the current intensity and there was a po-

sitive shift of the reduction peak potential. This result changes the reduction current which indicates interaction of Zn(II) with CT DNA.

Differential pulse voltammogram study. The differential pulse voltammograms of the glassy carbon electrode in solutions containing $[CuL(phen)_2]Cl_2$ both in the absence and presence of varying amounts of DNA are shown in Fig. 6.

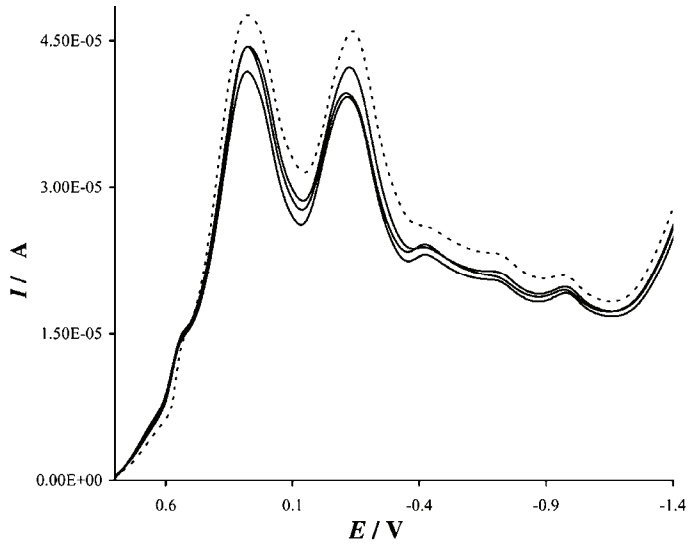

Fig.6. Differential pulse voltammograms of the glassy carbon electrode in solutions containing $[CuL(phen)_2]Cl_2$ in the absence (dash line) and presence (dark lines) of different concentrations (0 to 400 μM) of DNA.

The differential pulse voltammograms of the the glassy carbon electrode in solutions containing $[CuL(phen)_2]Cl_2$ showed that increasing the concentration of DNA resulted in a negative potential shift together with a significant decrease of the current intensity. The shift in potential is related to the ratio of the binding constants:

$$E_b - E_f = 0.0591\log (K_+/K_{2+}) \quad (2)$$

where E_b and E_f are the formal potential of the Cu(II)/Cu(I) complex couple in the bound and free forms, respectively. The ratio of the binding constants (K_+/K_{2+}) for DNA binding of the Cu(II)/Cu(I) couple of the complex was calculated and found to be less than unity. This indicates that the binding of the Cu(I) complex to DNA is small compared to that of the Cu(II) complex. The above electrochemical experimental results indicate that the Cu(II) complex binds to DNA molecules. The possible mechanism is:

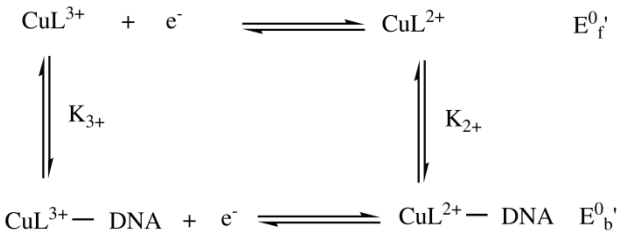

For a complex of the electro-active substance Zn^{2+} with DNA, the electrochemical reduction reactions can be divided into two steps:

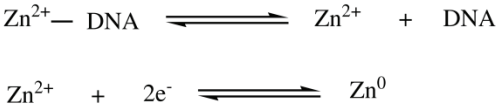

The dissociation constant (K_d) of the Zn^{2+}–CT-DNA complex was obtained using the following equation:

$$I_p^2 = \frac{K_d(I_{po}^2 - I_p^2)}{[DNA]} + I_{po}^2 - [DNA] \quad (3)$$

where K_d is the dissociation constant of the complex Zn(II)–DNA; I_{po}^2 is the reduction current of Zn(II) in the absence of CT-DNA; I_p^2 is the reduction current of Zn(II) in the presence of CT DNA; [DNA] is the concentration of added DNA in the solution. Using the above equation, the dissociation constant was determined (Table VI).

TABLE VI. Electrochemical parameters for the interaction of DNA with the Zn(II) complexes

Compound	E_p / V		I_p / A		$K_d \times 10^9$ / M^{-1}
	Free	Bound	Free	bound	
$[ZnL(phen)_2]Cl_2$	–0.989	–0.931	0.83	0.71	5.41
$[ZnL(bpy)_2]Cl_2$	–0.801	–0.789	0.89	0.78	5.44

The low values of the dissociation constant (Table VI) of Zn(II) ions are indispensable for the catalytic function and structural stability of zinc enzymes which participate in the replication, degradation, and translation of genetics of all species. Moreover, the Zn(II) ion probably not only interacted with the active site of the enzyme during these processes, as is already known in the literature,[18] but also with DNA.

Chemical nuclease activity

The cleavage efficiency of the complexes compared to that of the control is due to their efficient DNA-binding ability. DNA cleavage was controlled by relaxation of the supercoiled form of pUC19 DNA into the nicked circular form

and linear form. When pUC19 DNA is subjected to electrophoresis, the fastest migration will be observed for the supercoiled form (form I). If one strand is cleaved, the supercoils relax to produce the slower-moving open circular form (form II). If both strands are cleaved, the linear form (form III) will be generated that migrates between the other two forms.

DNA cleavage was analyzed by monitoring the conversion of supercoiled DNA (form I) to nicked DNA (form II) and linear DNA (form III) in the presence of the oxidant H_2O_2. The electrophoresis results are shown in Fig. 7.

From Fig. 7, it is evident that the complexes cleave DNA more efficiently in the presence of an oxidant (H_2O_2). This may be attributed to the formation of hydroxyl free radicals. The production of a hydroxyl radical due to the reaction between the metal complex and oxidant may be explained as shown below:

$$(\text{Ligand})Cu^{2+} + H_2O_2 \rightarrow (\text{Ligand})Cu^{3+} + OH\cdot + OH^-$$

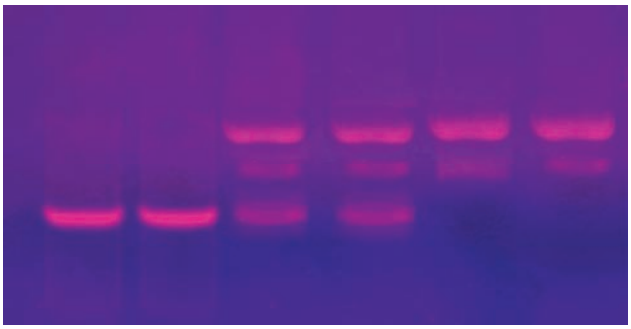

Fig. 7. Changes in the agarose gel electrophoretic pattern of pUC19 DNA induced by H_2O_2 and the Cu(II)/Zn(II) complexes. Lane 1, DNA alone; Lane 2, DNA + Ligand+ H_2O_2; Lane 3, DNA + $[CuL(phen)_2]Cl_2$ complex + H_2O_2; Lane 4, DNA + $[CuL(bpy)_2]Cl_2$ complex + H_2O_2; Lane 5, DNA + $[ZnL(phen)_2]Cl_2$ complex + H_2O_2; Lane 6, DNA + $[ZnL(bpy)_2]Cl_2$ complex + H_2O_2.

The OH· free radicals participate in the oxidation of the deoxyribose moiety, followed by hydrolytic cleavage of a sugar phosphate backbone. All the complexes showed pronounced nuclease activity in the presence of the oxidant H_2O_2, which may be due to the increased production of hydroxyl radicals. Control experiments using DNA alone resulted in no significant cleavage of pUC19 DNA, even after longer exposure times. From the observed results, it was concluded that all the complexes effectively cleaved the DNA as compared to control DNA. Furthermore, the presence of a smear in the gel diagram indicates the presence of radical cleavage.[19]

Antimicrobial screening

The synthesized ligand and its complexes were tested for their *in vitro* antimicrobial activity. They were tested against the bacteria S*taphylococcus aureus*,

Pseudomonas aeruginosa, *Escherichia coli*, *Staphylococcus epidermidis*, *Klebsiella pneumoniae* and the fungi *Aspergillus niger*, *Fusarium solani*, *Culvularia lunata*, *Rhizoctonia bataticola* and *Candida albicans*. The minimum inhibitory concentration *(MIC)* values of the investigated compounds are summarized in Tables VII and VIII. A comparison of the *MIC* value of L with those of the complexes indicates that the metal complexes exhibited higher antimicrobial activity than L and the control sample. Such increased activity of the complexes can be explained based on the Overtone's concept[20] and the Tweedy chelation theory.[21] According to the Overtone's concept of cell permeability, the lipid membrane that surrounds the cell favors the passage of only lipid-soluble materials, due to which liposolubility is an important factor that controls antimicrobial activity. On chelation, the polarity of the metal ion will be reduced due to the partial sharing of positive charges with donor groups. Furthermore, it increases the delocalization of π-electrons over the whole chelate ring and enhances the lipophilicity of the complexes. This increased lipophilicity enhances the penetration of the complexes into lipid membranes and the blocking of the metal binding sites in the enzymes of microorganisms. The results obtained from the antifungal and antibacterial tests showed that all the tested complexes were more active towards bacteria than fungi. Moreover, the copper complexes were more active than the zinc complexes against the tested microorganisms.

TABLE VII. Antibacterial studies of the investigated compounds (minimum inhibitory concentration×10^4, μmol/L)

Compound	*S. aureus*	*P. aeruginosa*	*E. coli*	*S. epidermidis*	*K. pneumoniae*
L	16.3	14.8	16.6	16.2	14.5
$[CuL(phen)_2]Cl_2$	1.4	1.6	1.2	1.0	1.9
$[CuL(bpy)_2]Cl2$	2.1	2.5	2.0	1.7	2.2
$[ZnL(phen)_2]Cl_2$	2.7	3.4	2.4	3.1	4.2
[ZnL(bpy)2]Cl2	3.6	4.8	2.5	3.9	4.4
Streptomycin	1.7	1.9	1.8	1.3	2.6

TABLE VIII. Antifungal studies of the investigated compounds (minimum inhibitory concentration×10^4, μmol/L)

Compound	*A. niger*	*F. solani*	*C. lunata*	*R. bataticola*	*C. albicans*
L	12.8	13.1	14.3	11.5	15.7
$[CuL(phen)_2]Cl_2$	2.0	2.6	3.9	3.8	4.9
$[CuL(bpy)_2]Cl_2$	3.2	3.4	4.3	4.1	5.3
$[ZnL(phen)_2]Cl_2$	5.1	5.3	5.9	6.1	6.4
$[CuL(phen)_2]Cl_2$	6.3	6.7	6.1	6.5	6.9
Nystatin	1.1	1.6	1.2	1.0	1.5

CONCLUSIONS

Four mixed ligand Cu(II) and Zn(II) complexes of an isatin-based Schiff base (L) and 1,10-phenanthroline/2,2'-bipyridine were synthesized and characterized. Elemental analyses, conductivity measurements and FAB-Mass spectrometry revealed the stoichiometry and composition of the complexes to be $[ML(bpy)_2/(phen)_2]Cl_2$. The FTIR, UV–Vis, ^{1}H-NMR, EPR spectra and magnetic measurements data confirmed the bonding features of the studied mixed ligand complexes. Electronic absorption spectroscopy, cyclic voltammetry, differential pulse voltammetry and viscometric studies demonstrated a considerable interaction between the complexes and calf-thymus DNA. The results of cleavage studies using pUC19 DNA showed that the complexes had higher nuclease activities than the isatin-based ligand. The *MIC* values against the growth of microorganisms are much larger for the complexes than those of the ligand and the control sample.

Acknowledgements. The authors express their sincere thanks to the College Managing Board, Principal and Head of the Department of Chemistry, VHNSN College, and Virudhunagar, India, for providing the necessary research facilities.

И З В О Д

СИНТЕЗА, КАРАКТЕРИЗАЦИЈА, ИНТЕРАКЦИЈА СА ДНК И АНТИМИКРОБНО ИЗУЧАВАЊЕ Cu(II) И Zn(II) КОМПЛЕКСА СА МЕШОВИТИМ ЛИГАНДИМА НА БАЗИ ИЗАТИНСКЕ И ПОЛИПИРИДИЛНЕ СТРУКТУРЕ

NATARAJAN RAMAN и SIVASANGU SOBHA

Research Department of Chemistry, VHNSN College, Virudhunagar-626 001, India

Синтетисано је неколико мешовито лигандних Cu(II)/Zn(II) комплекса коришћењем 3-(фенилимино)-1,3-дихидроиндол-2*H*-она (добијеног кондензацијом изатина и анилина) као примарног лиганда и 1,10-фенантролина (phen)/2,2'-бипиридина (bpy) као додатног лиганда и окарактерисано аналитички и спектроскопски елементалном анализом, мерењима магнетне сусцептибилности и моларне проводљивости, UV–Vis, IR, NMR и FAB масеним спектрима. Интеракција комплекса са ДНК телећег тимуса (CT) је изучавана помоћу апсорпционих спектара, мерењима цикличне волтаметрије, вискозности и гел-електрофорезом. Они имају апсорпциони хипохромизам и специфична вискозност расте у току везивања комплекса за ДНК телећег тимуса. Померања оксидо-редукционог потенцијала и промене у пиковима струје додатком ДНК су показане CV мерењима. Cu(II)/Zn(II) комплекси изазивају раскидање pUC19 ДНК из суперувијеног облика I у отворени кружни облик II и линеарни облик III. Комплекси су показали повећану антифунгалну и антибактеријску активност у односу на слободни лиганд.

(Примљено 20. октобра 2009, ревидирано 17. марта 2010)

REFERENCES

1. C. B. Spillane, M. N. V. Dabo, N. C. F. Fletcher, J. L. Morgan, R. Keen, I. Haq, N. J. Buurma, *J. Biol. Inorg. Chem.* **102** (2008) 673

2. M. S. Surendra Babu, P. G. Krishna, K. Hussain Reddy, G. H. Philip, *J. Serb. Chem. Soc.* 75 (2010) 61
3. D. S. Sigman, A. Mazumder, D. M. Perrin, *Chem. Rev*. **96** (1993) 2295
4. T. Ghosh, B. G. Maiya, A. Samanta, *J. Biol. Inorg. Chem*. **10** (2005) 496
5. N. J. Turro, J. K. Barton, D. A. Tomalia, *Acc. Chem. Res*. **24** (1991) 332
6. F. Q. Liu, Q. X. Wang, K. Jiao, F. F. Jian, G. Y. Liu, R. X. Li, *Inorg. Chim. Acta* **395** (2006) 1524
7. T. F. Tullis, *Metal–DNA chemistry*, ACS Symposium Series No. 402, American Chemical Society, Washington DC, 1989
8. J. K. Barton, *Science* **233** (1986) 727
9. S. P. Singh, S. K. Shukla, L. P. Awasthi, *Curr. Sci*. **52** (1983) 766
10. S. Arounaguiri, B. G. Maiya, *Inorg. Chem.* **38** (1999) 842
11. R. Pulimamidi, R. Nomula, R. Karnativ *Indian J. Chem.* **48** (2009) 1638
12. A. Kriza, C. Parnau, *Acta Chim. Slov*. **48** (2001) 445
13. J. A. Marmur, *J. Mol. Biol*. **3** (1961) 208
14. G. Speir, J. Csihony, J. M. Whalen, C. G. Pierpont, *Inorg. Chem.* **3** (1996) 3519
15. B. J. Hathaway, D. E. Billing, *Coord. Chem. Rev*. **5** (1970) 143
16. S. Sathyanarayana, J. C. Dabroniak, J. B. Chaires, *Biochemistry* **31** (1992) 9319
17. S. Sathyanarayana, J. C. Dabroniak, J. B. Chaires, *Biochemistry* **32** (1993) 2573
18. G. M. Blackburn, M. J. Gait, *Nucleic acid in chemistry and biology*, 2nd ed., Oxford University Press, New York, 1996
19. C. X. Zhang, S. J. Lippard, *Curr. Op. Chem. Biol*. **7** (2003) 481
20. Y. Anjaneyalu, R. P. Rao, *Synth. React. Inorg.-Org. Chem.* **16** (1986) 257
21. L. Mishra, V. H. Singh, *Indian J. Chem*. **32A** (1993) 446.